J. Indian Inst. Sci.
A Multidisciplinary Reviews Journal
ISSN: 0970-4140 Coden-JIISAD

REVIEW ARTICLE

Evidence for the Contrasting Magmatic Conditions in the Petrogenesis of A-type Granites of Phenai Mata Igneous Complex: Implications for Felsic Magmatism in the Deccan Large Igneous Province

K. R. Hari[1], M. P. Manu Prasanth[1], Vikas Swarnkar[2], Jami Vijaya Kumar[3] and Kirtikumar R. Randive[3]*

Abstract | We report contrasting magmatic conditions in the generation of anorogenic (A-type) felsic rocks from the Phenai Mata hill of Deccan Large Igneous Province. The felsic units in the present study area can be classified as granite, monzonite, quartz monzonite and granodiorite. The field as well as the geochemical evidences collectively indicate the mixing and mingling of contrasting magma compositions which were widely involved in the genesis of these anorogenic intrusions. Based on the anorogenic granite classification diagrams, it has been observed that the granite shows A1 type character whereas the monzonite, quartz monzonite and granodiorite exhibit A2 type characters. Both A1 and A2 type intrusions were compared with the associated basaltic andesites in the variation diagrams and found that the A1 type rocks exhibit a well-defined trend pointing towards a fractional crystallization process. The A2 type rocks do not exhibit any particular geochemical relation with the mafic rocks. Moreover, the A2 type rocks are characterized by negative Nb and Ta anomalies in the normalized diagrams indicating the involvement of crustal components. From the field and geochemical evidence, it can be presumed that the A1 type rocks represent the fractional crystallization sequence from a basaltic magma, whereas the A2 rocks might have been produced by the melting of the pre-existing crust or by the assimilation of crustal components into the mafic magma during ascent. These contrasting magmas along with the mafic magma variably interacted in the shallow crustal levels to form present-day field features in the Phenai Mata Igneous complex.

[1] School of Studies in Geology and Water Resource Management, Pt. Ravishankar Shukla University, Raipur, Chhattisgarh, India.
[2] Govt. Digvijay Autonomous P.G. College, Rajnandgaon, Chhattisgarh, India.
[3] Post-Graduate Department of Geology, RTM Nagpur University, Nagpur, India.
**krharigeology@gmail.com*

Springer IISc Press

1 Introduction

Large Igneous Province (LIP): Represents large accumulation of predominantly mafic intrusive and extrusive igneous rocks originated in a short span of time.

The large Igneous Provinces (LIPs) are generally known for its enormous basaltic magmatism and their economic potential.[1–3] The magma generation and diverse magmatic assemblages in the LIP record are intriguing and the magma generation processes involves mantle melting, creation of pathways for the melt transfer and wall rock interactions.[2, 4] However, while considering the complex nature of the magmatic systems, metasomatic reactions, compositional variations during ascent, branching and splitting of magma volumes are also needed to be evaluated. Moreover, the formation of intermediate magma chambers in the lower crustal regions and upper mantle discontinuities and other magmatic intrusions associated with LIPs are often accompanied by melt differentiation.[5] The LIPs may contain volumetrically minor amount silica saturated peralkaline volcanic rocks with anorogenic genetic characters, widely known as A-type granites. Even though these 'within plate' granitic magmatism is volumetrically small, they are important in understanding the evolution of the crust and they give important insights into the origin and diversity of magmas produced during the LIP events.[6] Generally, these granitic batholiths exhibit variable compositions and are thought to be formed either by the fractionation of a basaltic magma with or without crustal contamination or by the plume-induced melting of the crust. In some cases, compositionally diverse peraluminous, peralkaline and metaluminous A-type granitic intrusions in one particular region contemporaneous with the same LIP event is rather special because their sources could be different or they owe different petrogenetic histories.[7]

A-type granites: The granitoids generally occurred along the rift zones and within-stable continental plate setting.

The Deccan Large Igneous Province (Fig. 1), one of the largest igneous province in the world with an eruptive aerial extent of 106 km,[2] predominantly composed of tholeiitic basalts exhibit a wide range of isotopic ratios, major and trace element compositions.[8–10] The magmatic imprints of Deccan LIP indicate diverse rock assemblages which might have been produced by various modification processes such as fractional crystallization, crustal contamination, AFC, etc. However, the addition of continental lithospheric magmas into the main plume impulse could also be attributed to the wide compositional spectrum of Deccan LIP.[11, 12] The major derivative phases

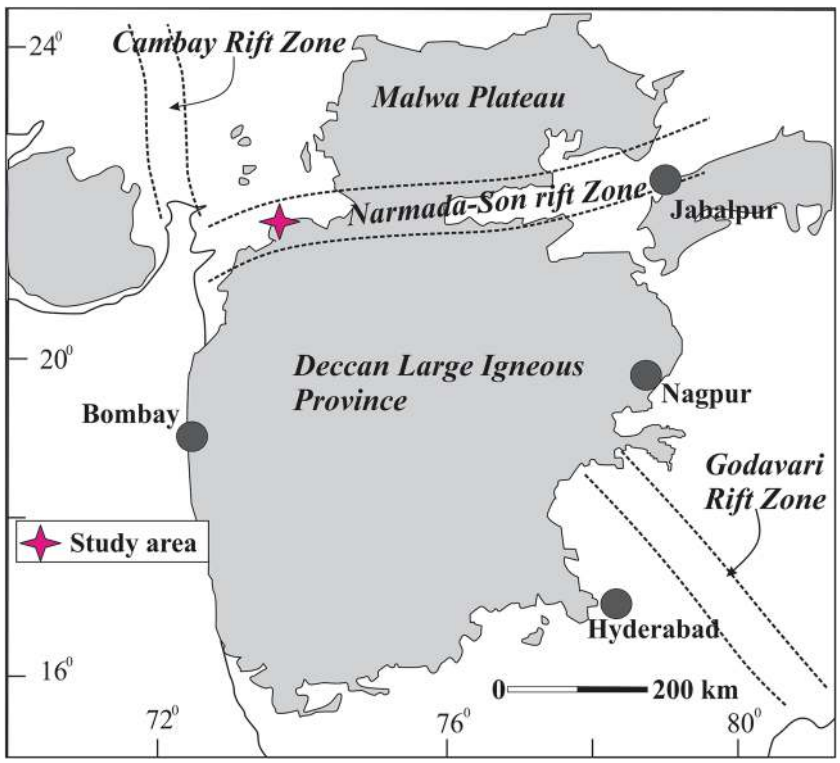

Figure 1: The generalized geological map of the Deccan Large Igneous Province showing the location of the Phenai Mata Igneous Complex[50].

such as alkali basalts, carbonatites, lamprophyres, and syenites were studied by various researchers[13–17] to evaluate the magmatic and metasomatic histories. However, considering the felsic volcanic imprints associated with the Deccan LIP, only the rhyolites have been studied in detail.[18, 19] The granites associated with Deccan LIP are minor and the majority of these A-type granites are confined to the Phenai Mata region. In the present study, we discuss the mineralogy and geochemistry of the A type granites and basic units from Phenai Mata Igneous Complex (PMIC) to deduce the petrogenetic history of PMIC.

2 Field Relations

The Chhotaudepur sub-province of Deccan LIP comprises mainly of two major igneous complexes namely, Ambadungar alkaline igneous complex in the southeast and the PMIC in the western part (Fig. 2). The stratigraphic succession of this area includes Bagh sandstone of Cretaceous age underlying the Deccan trap basaltic flows.[20, 21] The Ambadungar complex is mainly characterized by alkaline silicates and carbonatites. The main alkaline rocks of this terrane are nephelinite, tinguaite, etc. The presence of calcite-carbonatite and small plugs of red-brown ankeritic-carbonatite from Ambadungar complex is intriguing.[22, 23] The PMIC comprises of gabbro, granophyre, tholeiitic basalt, doleritic dykes and dyke-lets of granite.[24, 25] Felsic rocks constitute 1/4th of the Phenai Mata hill which mainly includes monazite, quartz monzonite, granite and granodiorite (Fig. 3a). The magma mixing and mingling processes are conspicuous in many portions of the Phenai Mata hill.[26] Majority of the

Magma mixing and mingling: Interaction of contrasting magma compositions, which is generally proposed in terms of mixing and mingling between a crustal melt and mafic material from the mantle that caused that melting.

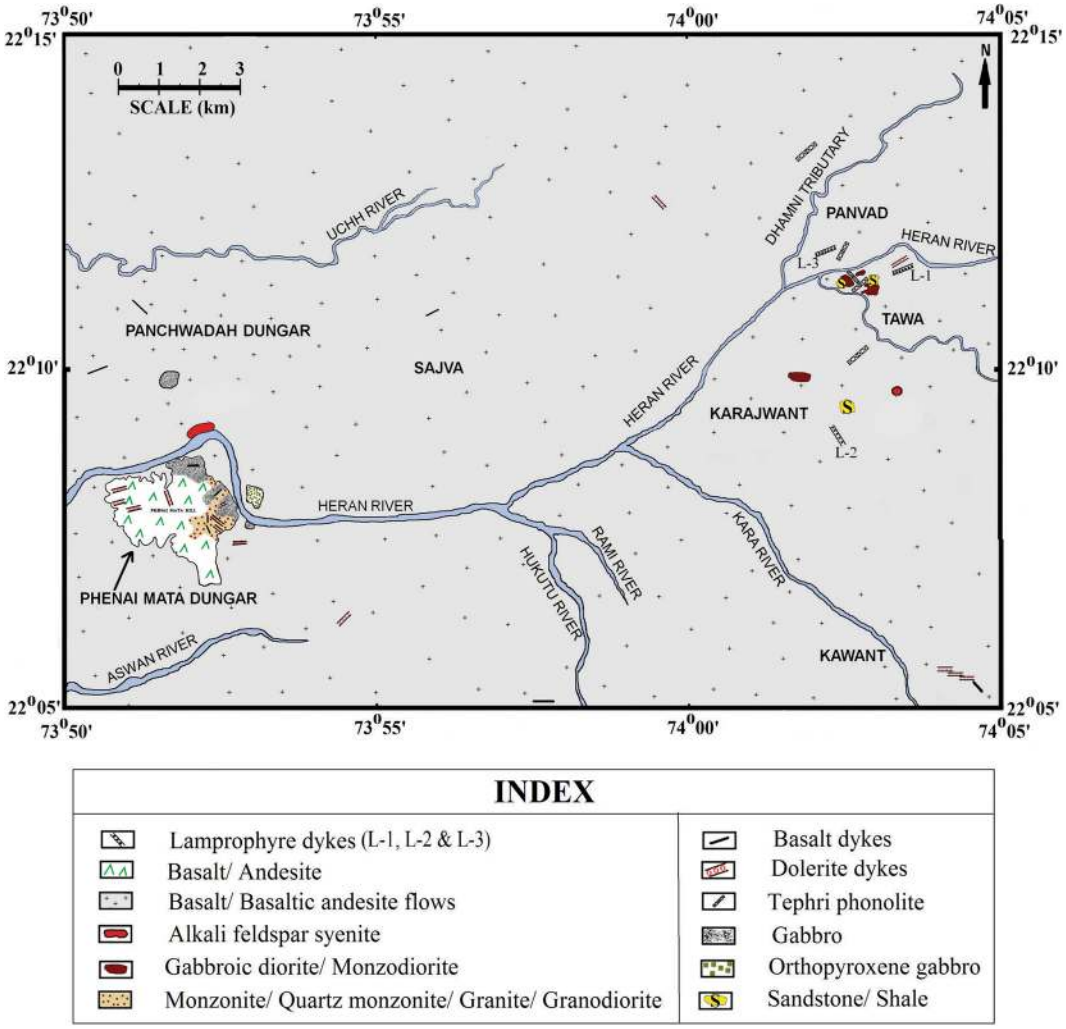

Figure 2: The regional geological map of the Phenai Mata Igneous complex and adjacent regions. (Modified after Hari et al.)[28]

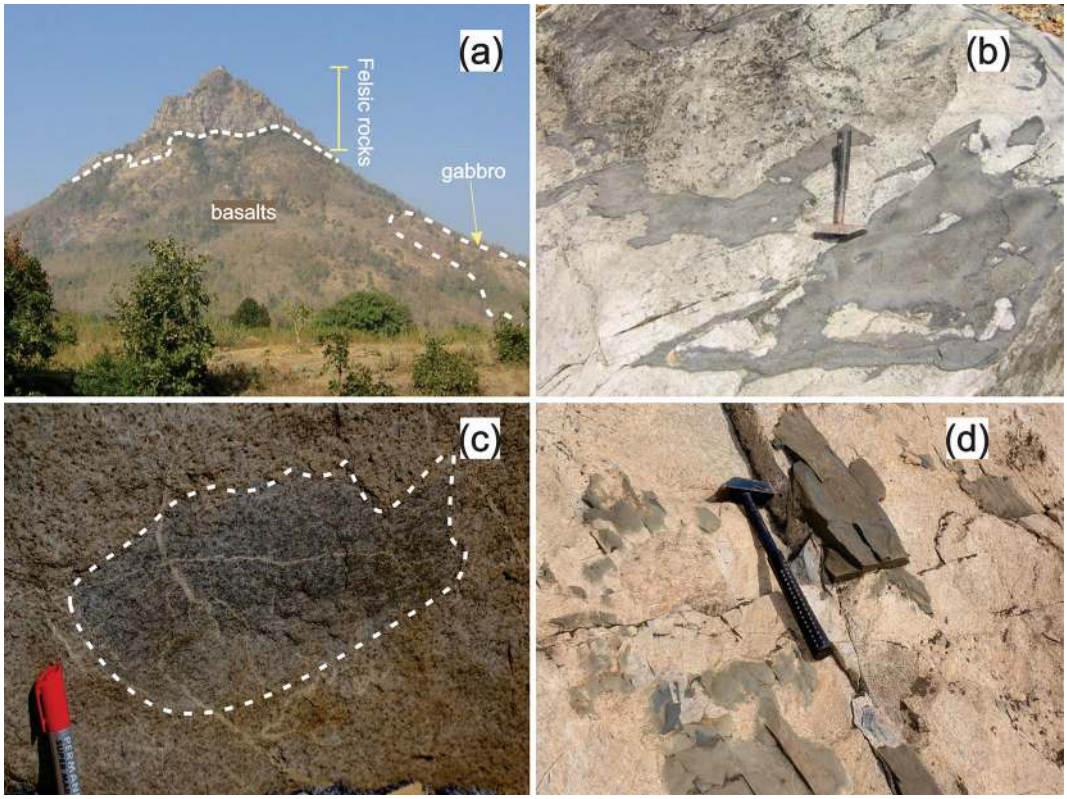

Figure 3: Field photographs showing **a** the panoramic view of the Phenai Mata hill showing the main mafic exposures and gabbroic rocks in the bottom and central portions and the top portion of the hill is mainly composed of felsic rocks. **b** interaction of felsic and mafic magmas in the top part of the PMIC, **c** moderately porphyritic mesocratic MME with in the granitic rocks of PMIC, **d** irregular syn-plutonic mafic dyke in the granitoids of the PMIC.

Phenai Mata region is characterized by the presence of xenoliths of mafic material in felsic rock indicating that the felsic magmatism followed was by the mafic magmatism or else contemporaneous eruption of both types of magma might have taken place. Gwalani et al.[27] reported basalt granophyre, hornblende dolerite, layered gabbro, gabbro, anorthosite and pulaskite from this area. Kumar[24] reported syenite, dolerite, lamprophyre, microgranite, tholeiitic gabbro, basalt and fine-grained gabbro from PMIC. Hari.et al.[28] reported alkali feldspar syenites with shoshonitic affinities from this area and proposed that they were derived from a metasomatically enriched mantle in an intracratonic rifting environment. Many fine-grained Mafic magmatic enclaves (MMEs) are found as inclusions in the host granites (Fig. 3b, c). Several syn-plutonic dykes (Fig. 3d) have also been demarcated from the PMIC. Hybrid rock zones where fine and coarse-grained mafic and felsic material being mixed is sporadically seen in the field. Texturally and mineralogically, diverse MMEs include densely porphyritic, lensoidal, ultramafic pegmatoidal, densely porphyritic mesocratic, sparsely porphyritic leucocratic, moderately porphyritic mesocratic, moderately porphyritic leucocratic, and felsic pegmatoidal types are noticeable in the PMIC.[26] The synplutonic dykes of PMIC exhibit feature such as necking down and changing trends, irregular, curvy and concave margins, ropy twists, intense back-veining and protuberances/dykelets within the granites.[26]

The felsic samples collected from PMIC are categorized as granite, granodiorite, monzonite and quartz monzonite as per the classification of Middlemost [29] (Fig. 4). The mafic volcanic rocks associated with the felsic rocks of the Pheani Mata hill are classified as basaltic andesites on the basis of TAS diagram (not shown). The mineral chemistry of felspars of granites, monzonites, and quartz monzonites are given in Tables 1, 2, and 3 respectively. Mineral chemistry of pyroxenes of monzonite is presented in Table 4. The major and trace element geochemistry of felsic rocks are presented in Table 5 and the major and trace

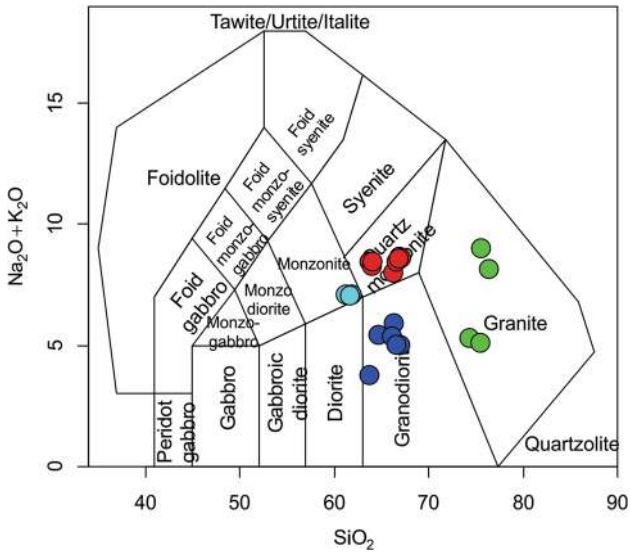

Figure 4: Classification of the felsic rocks from the PMIC as granites, granodiorites, monzonites and quartz-monzonites based on the classification of Middlemost[29].

Table 1: Mineral chemistry of feldspar from granite samples.

P-2	1	2	3	4	5	6	7
SiO_2	73.69	66.15	65.94	65.54	76.68	80.07	63.39
TiO_2	0.09	0.00	0.01	0.00	0.01	0.04	0.02
Al_2O_3	12.87	18.04	17.82	17.79	11.89	11.50	15.21
Cr_2O_3	0.00	0.00	0.00	0.00	0.00	0.03	0.02
FeO	0.05	0.07	0.00	0.06	0.01	0.08	0.02
MnO	0.00	0.07	0.00	0.02	0.08	0.09	0.03
MgO	0.01	0.00	0.00	0.01	0.00	0.00	0.01
CaO	0.01	0.16	0.24	0.19	0.01	0.39	0.12
Na_2O	1.48	4.02	5.12	3.89	1.30	3.05	3.39
K_2O	10.54	9.99	9.11	10.97	9.36	5.67	10.35
ZnO	0.01	0.00	0.00	0.00	0.01	0.00	0.14
P_2O_5	0.02	0.00	0.00	0.01	0.00	0.00	0.07
Total	98.77	98.48	98.24	98.48	99.33	100.91	92.79
Formula on the basis of 32 oxygen							
Si	13.210	12.113	12.096	12.082	13.503	13.650	12.376
Ti	0.012	0.000	0.001	0.000	0.001	0.005	0.003
Al	2.734	3.914	3.873	3.886	2.481	2.323	3.518
Cr	0.000	0.000	0.000	0.000	0.000	0.004	0.003
Fe	0.008	0.011	0.000	0.009	0.002	0.011	0.003
Mn	0.000	0.011	0.000	0.003	0.012	0.013	0.005
Mg	0.003	0.000	0.000	0.003	0.000	0.000	0.003
Ca	0.002	0.031	0.047	0.038	0.002	0.071	0.025
Na	0.514	1.427	1.821	1.390	0.444	1.008	1.283
K	2.411	2.334	2.132	2.580	2.103	1.233	2.578
Zn	0.001	0.000	0.000	0.000	0.001	0.000	0.020
P	0.003	0.000	0.000	0.002	0.000	0.000	0.012
Total	18.894	19.840	19.971	19.990	18.548	18.319	19.818

Table 2: Mineral chemistry of feldspar from Monzonite.

P-13	1	2	3	4	5
SiO_2	62.29	59.05	62.52	58.91	59.92
TiO_2	0.11	0.07	0.04	0.01	0.09
Al_2O_3	21.78	23.83	22.07	23.92	23.53
Cr_2O_3	0.00	0.02	0.00	0.00	0.04
FeO	0.42	0.49	0.43	0.49	0.48
MnO	0.00	0.01	0.00	0.00	0.00
MgO	0.01	0.01	0.00	0.00	0.10
CaO	4.31	6.83	4.35	7.17	6.29
Na_2O	8.62	7.05	8.29	6.95	7.36
K_2O	0.33	0.20	0.35	0.20	0.17
ZnO	0.00	0.09	0.00	0.00	0.00
P_2O_5	0.00	0.05	0.00	0.00	0.02
Total	97.87	97.70	98.07	97.64	98.01
Formula on the basis of 32 oxygen					
Si	11.273	10.789	11.277	10.766	10.884
Ti	0.015	0.010	0.005	0.001	0.012
Al	4.670	5.158	4.717	5.180	5.064
Cr	0.000	0.003	0.000	0.000	0.006
Fe	0.064	0.075	0.065	0.075	0.073
Mn	0.000	0.002	0.000	0.000	0.000
Mg	0.003	0.003	0.000	0.000	0.027
Ca	0.836	1.337	0.841	1.404	1.224
Na	3.025	2.497	2.899	2.463	2.592
K	0.076	0.0466	0.081	0.047	0.039
Zn	0.000	0.012	0.000	0.000	0.000
P	0.000	0.008	0.000	0.000	0.003
Total	19.962	19.932	19.884	19.936	19.922

element geochemistry of the mafic rocks are presented in Table 6.

3 Analytical Techniques

3.1 Mineral Chemistry

Chemical compositions of pyroxenes in the monzonites and the plagioclases in the quartz monzonite, granite and monzonite were analyzed using a CAMECA SX100 electron microprobe at the Institute of Mineralogy and Mineral Resources, Technical University of Clausthal, Germany. A beam current of 20 nA acceleration voltage of 20 kV and a beam diameter of 1 micron was used. Both natural and synthetic standards were employed and the details of the analytical procedures are given in Torab and Lehman.[30]

3.2 Whole Rock Major and Trace Elements

Major and trace element concentrations were analyzed using X-Ray Fluorescence Spectrometer (XRF) and Inductively Coupled Plasma-Mass Spectrometer (ICP-MS) at Wadia Institute of Himalayan Geology, Dehradun. The samples were crushed and pulverized with agate carbide ring grinder. The pressed pellets were used for the major element analysis. The open digestion method was used for the measurement of trace elements and REEs. Rock powders were dissolved in HF and HNO_3 in Teflon crucibles and heated over a hot plate for about 48 h. Further, the sample precipitate was used to prepare solutions for the measurement of trace element abundances using an ICPMS. The details of the analytical procedures are given in Singh et al.[31]

Table 3: Mineral chemistry of feldspar from Quartz monzonite.

P-1	1	2	3	4	5	6	7	8	9	10	11	12	13
SiO_2	59.42	60.42	59.75	60.21	60.21	60.33	59.86	61.16	60.79	61.01	60.46	60.77	61.46
TiO_2	0.00	0.00	0.04	0.00	0.10	0.02	0.04	0.00	0.00	0.05	0.03	0.01	0.02
Al_2O_3	23.50	23.18	23.34	23.51	23.28	23.87	23.10	23.90	23.46	23.71	23.79	23.41	22.89
Cr_2O_3	0.00	0.02	0.01	0.00	0.00	0.04	0.01	0.03	0.00	0.00	0.01	0.00	0.02
FeO	0.37	0.29	0.43	0.34	0.32	0.35	0.28	0.27	0.36	0.44	0.33	0.40	0.38
MnO	0.06	0.00	0.00	0.00	0.06	0.00	0.00	0.00	0.00	0.04	0.00	0.07	0.00
MgO	0.01	0.01	0.01	0.00	0.01	0.01	0.01	0.00	0.02	0.01	0.01	0.01	0.00
CaO	6.48	6.09	6.27	6.26	5.95	6.67	6.27	6.27	6.24	6.24	6.43	6.12	5.39
Na_2O	7.46	7.74	7.63	7.34	7.78	7.22	7.72	7.38	7.38	7.49	7.23	7.65	7.97
K_2O	0.36	0.35	0.36	0.36	0.28	0.36	0.45	0.40	0.28	0.40	0.37	0.32	0.31
ZnO	0.06	0.21	0.03	0.00	0.00	0.02	0.10	0.00	0.00	0.00	0.00	0.07	0.06
P_2O_5	0.00	0.00	0.04	0.00	0.00	0.00	0.03	0.02	0.00	0.03	0.01	0.04	0.00
Total	97.72	98.32	97.90	98.03	97.99	98.89	97.86	99.43	98.54	99.42	98.66	98.87	98.51
Formula on the basis of 32 oxygen													
Si	10.852	10.953	10.889	10.927	10.937	10.867	10.918	10.935	10.965	10.929	10.902	10.950	11.079
Ti	0.000	0.000	0.006	0.000	0.014	0.003	0.006	0.000	0.000	0.007	0.004	0.001	0.003
Al	5.085	4.979	5.040	5.055	5.010	5.094	4.992	5.063	5.014	5.032	5.082	4.998	4.889
Cr	0.000	0.003	0.002	0.000	0.000	0.006	0.002	0.004	0.000	0.000	0.001	0.000	0.003
Fe	0.057	0.044	0.066	0.052	0.049	0.053	0.043	0.040	0.054	0.066	0.050	0.060	0.057
Mn	0.009	0.000	0.000	0.000	0.009	0.000	0.000	0.000	0.000	0.006	0.000	0.011	0.000
Mg	0.003	0.003	0.003	0.000	0.003	0.003	0.003	0.000	0.005	0.003	0.003	0.003	0.000
Ca	1.268	1.183	1.224	1.217	1.158	1.287	1.225	1.201	1.206	1.198	1.242	1.182	1.041
Na	2.642	2.721	2.696	2.583	2.740	2.522	2.730	2.559	2.581	2.601	2.528	2.673	2.786
K	0.084	0.081	0.084	0.083	0.065	0.083	0.105	0.091	0.064	0.091	0.085	0.074	0.071
Zn	0.008	0.028	0.004	0.000	0.000	0.003	0.014	0.000	0.000	0.000	0.000	0.009	0.008
P	0.000	0.000	0.006	0.000	0.000	0.000	0.005	0.003	0.000	0.005	0.002	0.007	0.000
Total	20.007	19.994	20.012	19.917	19.984	19.920	20.035	19.894	19.889	19.933	19.897	19.960	19.937

Table 4: Mineral chemistry of pyroxene from Monzonite.

P-13	1	2	3	4	5	6	7	8	9
SiO_2	52.70	53.34	51.03	51.10	51.26	50.95	51.78	51.64	51.90
TiO_2	0.40	0.51	0.22	0.51	0.51	0.51	0.47	0.48	0.52
Al_2O_3	2.19	1.80	1.03	1.44	1.49	1.49	1.38	1.26	1.28
Cr_2O_3	0.00	0.00	0.03	0.00	0.00	0.06	0.00	0.04	0.02
FeO	10.73	10.36	11.05	11.39	11.23	11.00	11.17	11.51	11.47
MnO	0.55	0.72	0.95	0.58	0.51	0.55	0.50	0.63	0.69
MgO	16.56	16.96	12.64	13.96	13.97	14.00	14.05	13.85	13.83
CaO	10.65	10.22	18.73	18.09	18.57	18.48	17.95	17.87	17.89
Na_2O	1.58	1.74	0.66	0.30	0.27	0.29	0.27	0.27	0.27
K_2O	0.56	0.49	0.16	0.01	0.02	0.00	0.02	0.00	0.00
ZnO	0.14	0.07	0.06	0.03	0.00	0.09	0.12	0.00	0.18
P_2O_5	0.00	0.01	0.00	0.01	0.00	0.00	0.03	0.04	0.00
Total	96.07	96.21	96.57	97.42	97.83	97.44	97.74	97.59	98.05
Formula on the basis of 6 oxygen									
Si	2.009	2.020	1.988	1.965	1.962	1.959	1.979	1.980	1.981
Ti	0.011	0.010	0.007	0.015	0.015	0.015	0.014	0.014	0.015
Al	0.099	0.080	0.048	0.066	0.068	0.068	0.063	0.057	0.058
Cr	0.000	0.000	0.001	0.000	0.000	0.002	0.000	0.001	0.001
Fe	0.342	0.330	0.360	0.366	0.360	0.354	0.357	0.369	0.366
Mn	0.018	0.020	0.031	0.019	0.017	0.018	0.016	0.021	0.022
Mg	0.941	0.960	0.734	0.800	0.797	0.802	0.800	0.791	0.787
Ca	0.435	0.420	0.782	0.745	0.762	0.761	0.735	0.734	0.732
Na	0.117	0.130	0.050	0.022	0.020	0.022	0.020	0.020	0.020
K	0.027	0.020	0.008	0.001	0.001	0.000	0.001	0.000	0.000
Zn	0.004	0.000	0.002	0.001	0.000	0.003	0.003	0.000	0.005
P	0.000	0.000	0.000	0.000	0.000	0.000	0.001	0.001	0.000
Total	4.003	3.998	4.010	4.000	4.000	4.003	3.988	3.987	3.986

4 Petrography and Mineral Chemistry

The major mineral assemblages of the granite include alkali feldspars, plagioclases and quartz. The accessory minerals include biotite, hornblende, titanite, apatite and zircon (Fig. 5b). Some portions of the granites contain augite to sub calcic augite pyroxene grains. In the feldspar classification diagram (Fig. 6a), all the dominant feldspars from the granites plot in the sanidine field (Or_{53-83} Ab_{17-46} $An_{0.07-3}$). Intergrowth textures like myrmekitic, poikilitic and perthite have also been identified in the granites. Zoning is observed in some plagioclase grains in the granites and granodiorites. Plagioclases observed in the granodiorites are partially sericitized and saussuritized. Micrographic texture (Fig. 5d) is noticeable in monzonite only. Interlocking arrangement of quartz and feldspar are noticeable in most of the samples and it might have been originated by the simultaneous crystallization of quartz and plagioclase from a silicate melt with the presence of a hydrous phase. Chlorite minerals are seen as accessories along with biotite in most of the monzonite samples. The pyroxenes (Fig. 5d) of monzonite is classified as augite (Fig. 6b). The presence of magnetite and titanomagnetite are also noticeable in the monzonite and quartz monzonite. The quartz monzonite samples are characterized by abundant plagioclase phenocrysts (Fig. 5a, c). Most of the plagioclases are sericitized and saussuritized. In the groundmass of quartz monzonite samples, chlorite minerals are found as accessories along with few biotite flakes. Silicate liquid immiscible globules are noted in many sections of quartz monzonite (Fig. 5c). Some xenolith fragments exhibit trachytic texture and

Table 5: The major and trace element geochemistry of monzonites, quartz monzonites, granites and granodiorites from the PMIC.

	Monzonite				Quartz monzonite					
Sample	P-13a	P-13b	P-13c	P-13d	K-2a	K-2b	K-2c	P-1a	P-1b	P-4a
SiO_2	60.83	60.39	60.73	60.73	62.66	62.66	62.68	66.19	66.03	66.15
Al_2O_3	15.68	15.81	15.56	15.58	15.95	15.93	15.95	13.46	13.35	13.44
Fe_2O_3	7.56	7.52	7.58	7.57	5.34	5.33	5.33	6.73	6.75	6.41
MnO	0.11	0.12	0.1	0.1	0.13	0.13	0.11	0.14	0.14	0.13
MgO	2.94	2.94	2.87	2.87	1.65	1.46	1.62	0.18	0.72	0.13
CaO	3.6	3.61	3.54	3.54	3.46	3.54	3.39	2.55	2.53	2.8
Na_2O	3.31	3.34	3.28	3.27	3.78	3.66	3.93	4.12	4.1	4.44
K_2O	3.51	3.56	3.5	3.51	4.38	4.35	4.34	4.31	4.31	4.22
TiO_2	0.77	0.79	0.75	0.76	0.79	0.78	0.75	0.65	0.65	0.63
P_2O_5	0.28	0.28	0.27	0.28	0.3	0.3	0.31	0.26	0.25	0.24
Sc	12.99	9.86	12.45	14.25	12.35	10.22	12.35	10.16	10.59	9.59
V	10.75	7.74	11.25	11.98	13.56	10.56	13.33	27.07	32.40	29.63
Cr	26.88	16.48	22.14	19.24	19.14	11.14	16.58	93.10	94.40	76.20
Co	10.31	7.03	9.71	10.56	8.37	6.60	8.17	9.33	9.66	8.09
Ni	13.02	2.39	4.01	3.27	1.75	1.15	1.65	8.49	9.17	8.37
Cu	1.95	0.51	1.59	0.78	0.42	0.30	0.41	25.47	25.79	20.99
Zn	87.57	33.50	89.28	54.84	43.90	33.56	44.76	105.80	103.67	74.76
Ga	36.06	25.72	32.73	38.67	34.70	27.19	33.45	22.14	23.10	21.73
Rb	322.63	220.17	286.97	332.29	278.49	222.41	267.76	224.03	234.95	209.63
Sr	207.52	147.91	197.80	222.70	181.93	146.08	176.55	228.31	238.50	231.07
Y	120.77	85.58	108.88	125.90	110.33	86.73	106.60	70.45	74.02	69.90
Zr	329.05	275.23	320.03	381.49	1395.61	822.36	1205.23	171.63	170.38	156.44
Nb	111.00	87.61	101.60	126.41	101.85	83.73	102.64	74.24	80.82	67.90
Cs	4.41	2.78	3.53	4.13	4.00	3.15	3.91	2.80	2.95	2.38
Ba	545.74	400.40	521.31	598.61	477.38	385.54	476.78	296.05	308.90	284.73
La	177.02	122.29	154.25	187.44	154.11	120.35	149.95	97.82	102.33	101.42
Ce	329.68	231.17	290.98	351.06	283.63	223.65	276.39	170.82	179.42	173.01
Pr	32.95	23.50	29.46	35.22	28.73	22.86	27.99	16.40	17.06	16.47
Nd	121.33	86.60	108.32	130.21	105.46	83.92	102.34	67.50	70.45	67.73
Sm	20.83	14.74	18.78	22.52	18.35	14.82	18.10	11.61	12.04	11.70
Eu	1.97	1.46	1.90	2.18	1.82	1.48	1.79	2.41	2.46	2.40
Gd	21.21	15.22	18.93	22.30	18.82	14.77	17.74	12.50	13.07	12.49
Tb	3.16	2.26	2.82	3.37	2.78	2.22	2.70	1.56	1.61	1.56
Dy	19.89	14.14	17.92	20.83	18.21	14.23	17.30	10.25	10.54	10.05
Ho	2.33	1.67	2.10	2.48	2.15	1.69	2.06	2.20	2.24	2.14
Er	8.29	6.00	7.58	8.80	7.69	6.09	7.35	6.00	6.38	6.07
Tm	1.08	0.73	0.96	1.09	0.98	0.77	0.93	0.73	0.74	0.72
Yb	11.06	7.81	9.91	12.00	10.22	8.18	10.17	4.29	4.53	4.21
Lu	1.80	1.29	1.61	1.91	1.70	1.33	1.66	0.91	0.92	0.87
Hf	9.19	7.62	8.48	10.41	36.68	21.60	31.64	4.07	3.97	3.75
Ta	8.05	4.09	6.28	7.66	6.44	5.65	7.07	4.88	5.26	2.84
Pb	30.14	14.49	22.78	20.36	11.51	9.28	11.43	3.08	2.98	4.09
Th	53.69	37.31	48.43	56.39	50.02	38.72	49.73	26.68	27.88	26.92
U	12.35	7.70	11.36	11.10	11.78	8.62	11.08	2.84	2.84	2.93

Table 5: continued

Sample	Quartz monzonite			Granite					
	P-4b	P-7a	P-7b	P-2a	P-2b	P-5a	P-5b	V-02	V-15
SiO_2	66.13	65.92	65.94	73.82	73.83	75.32	75.31	73.9	73.4
Al_2O_3	13.43	13.45	13.42	12.07	12.08	12.28	12.2	12.64	12.89
Fe_2O_3	6.44	7	6.97	1.99	2	2.1	2.1	2.3	2.65
MnO	0.13	0.15	0.15	0.02	0.02	0.02	0.02	0.03	0.03
MgO	0.15	1	1.01	0.5	0.51	0.17	0.18	0.85	1.38
CaO	2.8	2.48	2.49	0.45	0.45	0.49	0.5	2.48	2.45
Na_2O	4.43	3.85	3.84	3.17	3.16	2.59	2.58	2.97	3.08
K_2O	4.22	4.13	4.13	5.78	5.77	5.46	5.46	2.04	2.15
TiO_2	0.64	0.68	0.69	0.17	0.17	0.22	0.23	0.72	0.77
P_2O_5	0.24	0.26	0.26	0.06	0.06	0.05	0.05	0.04	0.05
Sc	9.84	10.63	10.45	4.61	4.15	5.34	5.39	5.76	7.98
V	27.77	28.62	37.00	18.62	12.87	14.98	23.62	15.67	16.46
Cr	80.60	72.00	78.38	68.87	59.37	41.09	75.52	25.56	31.05
Co	8.32	9.31	8.93	2.88	2.59	2.77	2.46	1.74	1.99
Ni	8.03	8.09	9.57	6.38	4.73	5.67	5.84	5.18	2.70
Cu	22.18	23.24	28.77	17.97	19.66	12.19	12.86	11.69	14.47
Zn	81.92	78.88	86.69	33.98	30.74	32.66	30.29	42.10	28.44
Ga	22.08	22.58	21.36	17.90	17.10	18.95	19.07	16.90	18.29
Rb	212.85	219.87	206.37	285.56	272.60	269.76	278.56	126.79	125.94
Sr	240.32	225.83	222.58	61.99	52.63	50.89	42.01	62.76	42.84
Y	71.64	76.27	73.43	32.52	30.14	28.18	27.12	42.45	41.56
Zr	168.23	140.15	133.57	60.37	53.57	72.81	72.11	45.99	57.25
Nb	76.87	83.34	75.87	19.34	16.69	23.60	21.22	21.81	23.91
Cs	2.44	2.46	2.36	2.08	2.00	3.14	3.29	2.79	1.50
Ba	294.09	299.78	295.13	163.02	150.78	114.96	107.96	359.48	514.01
La	104.74	109.34	107.05	66.41	62.44	90.54	90.51	71.92	86.61
Ce	179.92	192.29	183.80	125.62	118.04	162.03	161.65	111.32	143.79
Pr	16.94	18.33	17.44	12.21	11.54	15.52	15.46	14.64	17.49
Nd	69.64	76.14	72.47	49.39	46.35	62.94	63.66	54.10	63.06
Sm	11.93	13.07	12.35	8.63	8.19	10.49	10.65	9.38	10.50
Eu	2.50	2.57	2.55	0.83	0.73	0.83	0.76	0.73	0.79
Gd	12.97	14.23	13.44	8.47	7.88	10.58	10.28	9.62	10.63
Tb	1.60	1.73	1.67	0.94	0.88	1.04	1.04	1.54	1.61
Dy	10.35	11.08	10.91	5.24	4.94	5.10	4.91	6.25	6.26
Ho	2.22	2.37	2.33	1.02	0.97	0.88	0.89	1.25	1.21
Er	6.24	6.77	6.51	2.80	2.64	2.43	2.36	4.46	4.30
Tm	0.74	0.80	0.78	0.31	0.29	0.24	0.24	0.62	0.54
Yb	4.42	4.70	4.64	1.92	1.67	1.50	1.39	3.93	3.28
Lu	0.90	0.98	0.96	0.38	0.34	0.30	0.29	0.57	0.48
Hf	4.11	3.51	3.38	1.72	1.46	2.04	2.00	1.45	1.68
Ta	3.56	5.86	4.88	1.69	1.65	2.10	1.76	2.01	2.03
Pb	4.06	3.17	3.35	3.81	4.00	5.03	5.12	7.41	6.56
Th	27.49	28.42	26.92	36.83	37.49	39.28	38.35	38.40	42.94
U	2.97	2.87	2.80	4.88	3.85	2.61	2.63	3.95	5.92

Table 5: continued

Sample	V-01	V-06	V-07	V-09	V-11	V-14
Granodiorite						
SiO_2	66	65.4	63.7	65.8	65.4	62.4
Al_2O_3	13.46	13.35	13.46	14.75	13.64	14.06
Fe_2O_3	6.14	6.33	6.89	5.94	7.17	9.16
MnO	0.08	0.09	0.09	0.05	0.1	0.09
MgO	2.68	3.17	3.53	1.66	1.4	3.28
CaO	3.8	3.78	3.81	3.7	3.87	4.01
Na_2O	3.17	3.45	3.58	2.65	3.87	1.84
K_2O	1.77	1.74	1.68	2.29	1.9	1.79
TiO_2	1.04	1.05	1.08	1.24	1.1	1.63
P_2O_5	0.2	0.2	0.22	0.18	0.2	0.15
Sc	8.00	8.28	8.42	11.56	13.24	14.33
V	27.34	29.55	30.51	56.79	30.73	71.48
Cr	21.66	26.93	27.71	45.71	32.14	29.43
Co	6.50	7.45	7.95	6.99	9.27	13.09
Ni	7.35	6.13	3.38	5.28	8.34	6.22
Cu	11.52	17.43	15.17	21.53	20.14	11.58
Zn	67.01	69.27	76.03	70.22	262.88	108.18
Ga	18.88	19.24	19.75	23.16	27.13	23.00
Rb	118.26	101.49	97.01	107.19	144.99	97.67
Sr	126.76	137.05	142.17	172.46	231.26	164.02
Y	70.22	59.84	62.09	32.78	82.55	31.54
Zr	131.25	136.77	142.43	54.76	116.63	116.61
Nb	60.94	61.67	61.30	61.50	95.14	56.10
Cs	1.99	1.06	1.13	1.61	2.20	3.02
Ba	791.12	876.97	825.35	945.19	1512.34	589.47
La	73.54	73.45	73.03	70.43	102.10	62.57
Ce	119.11	120.28	120.48	124.15	168.28	109.58
Pr	14.58	14.35	14.47	15.39	20.32	14.02
Nd	53.39	52.74	53.37	60.73	75.61	55.05
Sm	9.36	9.11	9.19	10.58	12.90	9.75
Eu	1.36	1.49	1.56	2.66	2.56	2.48
Gd	10.48	9.89	9.93	10.16	13.91	9.30
Tb	1.82	1.68	1.72	1.50	2.36	1.40
Dy	8.20	7.59	7.83	5.53	10.65	5.09
Ho	1.82	1.63	1.70	1.00	2.30	0.96
Er	6.57	6.04	6.14	2.98	8.42	3.11
Tm	0.99	0.88	0.92	0.35	1.22	0.38
Yb	5.97	5.48	5.76	2.01	7.53	2.16
Lu	0.88	0.81	0.85	0.24	1.12	0.31
Hf	3.32	3.44	3.58	1.36	3.14	2.97
Ta	3.97	3.72	4.11	3.83	5.77	2.91
Pb	3.62	4.88	5.40	5.31	5.33	4.39
Th	30.37	29.94	29.78	18.32	35.24	15.07
U	5.94	6.47	6.55	2.16	6.12	1.94

Table 6: Major and trace element geochemistry of the mafic rocks of PMIC.

Sample	P-6A	P-6B	V-10
SiO_2	56.91	56.89	57.10
Al_2O_3	15.34	15.62	14.18
Fe_2O_3	11.36	11.34	10.71
MnO	0.12	0.12	0.11
MgO	2.43	2.43	3.71
CaO	5.66	5.66	6.84
Na_2O	2.29	2.28	2.70
K_2O	2.75	2.75	1.44
TiO_2	1.1	1.1	1.57
P_2O_5	0.3	0.3	0.31
Sum	98.26	98.49	98.68
Sc	19.757	19.764	21.123
V	141.790	145.335	173.363
Cr	82.247	73.403	23.357
Co	24.766	24.526	23.649
Ni	23.084	22.127	5.96
Cu	42.877	44.382	17.109
Zn	83.329	85.826	81.698
Ga	21.161	20.682	19.559
Rb	114.210	112.440	55.093
Sr	361.622	349.722	295.552
Y	49.308	47.904	43.662
Zr	80.904	74.256	46.459
Nb	46.154	43.893	39.314
Cs	1.987	1.949	1.824
Ba	335.698	329.348	909.931
La	79.353	80.024	55.695
Ce	135.258	135.683	91.262
Pr	13.528	13.137	11.124
Nd	57.557	56.360	43.482
Sm	9.782	9.566	7.621
Eu	2.494	2.479	1.967
Gd	10.594	10.669	8.127
Tb	1.255	1.241	1.375
Dy	7.654	7.522	5.917
Ho	1.535	1.490	1.231
Er	4.036	3.978	4.369
Tm	0.459	0.444	0.616
Yb	2.578	2.462	3.73
Lu	0.531	0.525	0.561
Hf	1.958	1.932	1.241
Ta	3.040	2.858	2.325
Pb	3.347	3.339	3.965
Th	8.202	8.337	13.937
U	0.950	0.947	2.095

generally altered to sericite (Fig. 5b). The abundant granophyric texture observed in some of the samples point towards an anorogenic setting which are related to the continental rift environment.[32,33]

The basaltic andesites of the PMIC mainly composed of pyroxenes and plagioclases as phenocrysts and the groundmass are generally composed of plagioclase, clinopyroxene, glass and opaques (Fig. 5e, f).

5 Whole Rock Geochemistry

The granite samples exhibit higher SiO_2 (73.4–75.32 wt%) contents relative to the granodiorite (62.4–66 wt%), monzonite (~60 wt%) and quartz monzonite (62.66–66.19 wt%). All the samples exhibit relatively low MgO values (monzonite: 2.87–2.94 wt%; quartz monzonite: 0.13–1.65 wt%; granite: 0.5–1.38 wt% and granodiorite: 1.4–3.28 wt%, respectively) (Table 5). In the variation diagrams (Fig. 7), all major elements show a general decreasing trend with the increase in SiO_2 content. When the felsic rocks of PMIC are compared with the associated mafic rocks of PMIC, all the samples except the granites exhibit a linear correlation. Feldspar fractionation is evident from the decreasing Al_2O_3, CaO and Sr with the SiO_2 increase. The Fe–Ti oxide fractionation is evident by the progressive decrease in TiO_2 and Fe_2O_3 with SiO_2 increase (Fig. 7). All the felsic samples exhibit enriched REE (Fig. 8) with low concentrations of Co, Sc, Cr (11.14–94.39 ppm), Ni (1.15–9.57), and Eu (0.73–2.65 ppm). The REE chondrite and primitive mantle normalized diagrams of different felsic units are shown in Fig. 8. In the primitive mantle normalized multi-element diagram (Fig. 8), granites exhibit Rb, Ta, Nb, Sr, Hf, Zr, Ti negative anomalies and Th, La, Nd, and Zr positive anomalies, whereas granodiorite, monzonite and quartz monzonite exhibit Ba, Sr, Hf, Zr, and Ti negative anomalies. The granite has the lowest whereas monzonite has the highest REE concentrations. In all the cases, prominent negative Eu anomaly is noticeable indicating plagioclase fractionation.

The mafic rocks of Phenai Mata exhibit low SiO_2 (56.8–57.1 wt%) and high Fe_2O_3(10.7–11.3 wt%), Al_2O_3 (14.1–15.6 wt%) and TiO_2 (1.1–1.57 wt%) contents (Table 6). In the chondrite normalized REE diagram, mafic samples exhibit LREE enrichment relative to the HREE (Fig. 9a). In the primitive mantle normalized multi-element diagram, the samples exhibit Pr, Zr and Ti negative anomalies and La, Nb, Ta, Nd and Gd positive anomalies (Fig. 9b). When the mafic

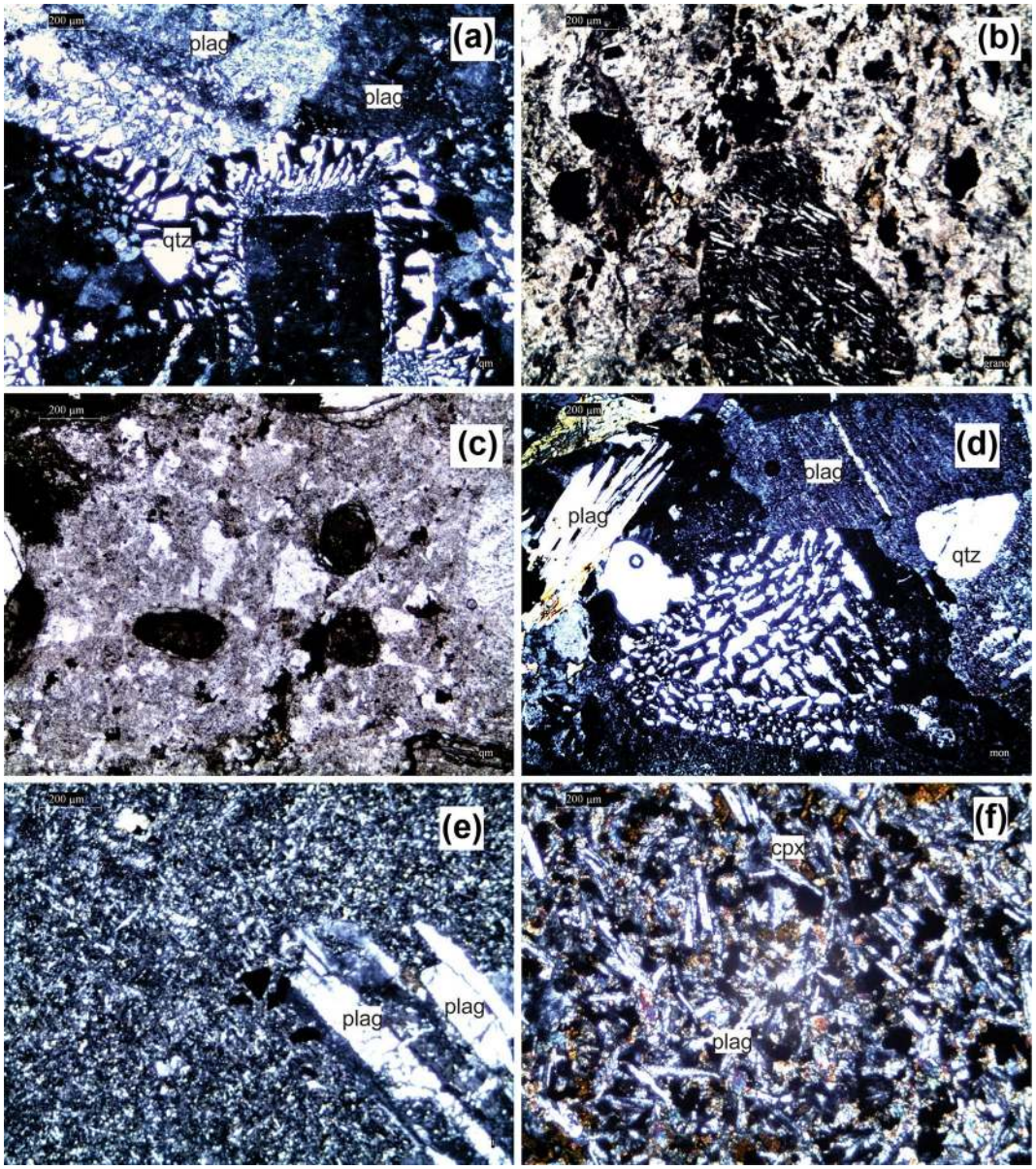

Figure 5: **a** Granophyric texture in the quartz-monzonite show Micrographic groundmass surrounds feldspar phenocryst fragment. **b** The pyroxene grain exhibit assimilated fragments from the felsic host. **c** Presence of silicate liquid immiscibility globules in the monzonite sample. **d** The granophyric texture in the monzonite radiating fringe of feldspar grains and the growth of granophyre. **e**, **f** Basalts from the PMIC exhibit flow textures with plagioclases and clinopyroxenes.

samples of PMIC were compared with the basalts from the chhotaudepur province, and found that the REE and primitive mantle normalized multi-element patterns are consistent with the reported data[34].

6 Discussions

In the 1000*Ga/Al vs. Ce and 1000*Ga/Al vs. Zn classification diagrams[32] (Fig. 10) all the felsic samples from the PMIC plot in the A-type granites field. Further, when the felsic samples were plotted in the granitoid discrimination diagrams proposed by Pearce et al.[35] and Whalen et al.[32], all the samples fall on WPG (within plate granitoid) field (Fig. 11). Generally, A-type granitoids will be enriched in LREE (La/Yb = 12.3–37.3, except sample P-5b with 65.1) and will have relatively flat to somewhat depleted HREE (Ce/Yb = 2.2–5.5) with prominent negative Eu anomalies in the chondrite normalized

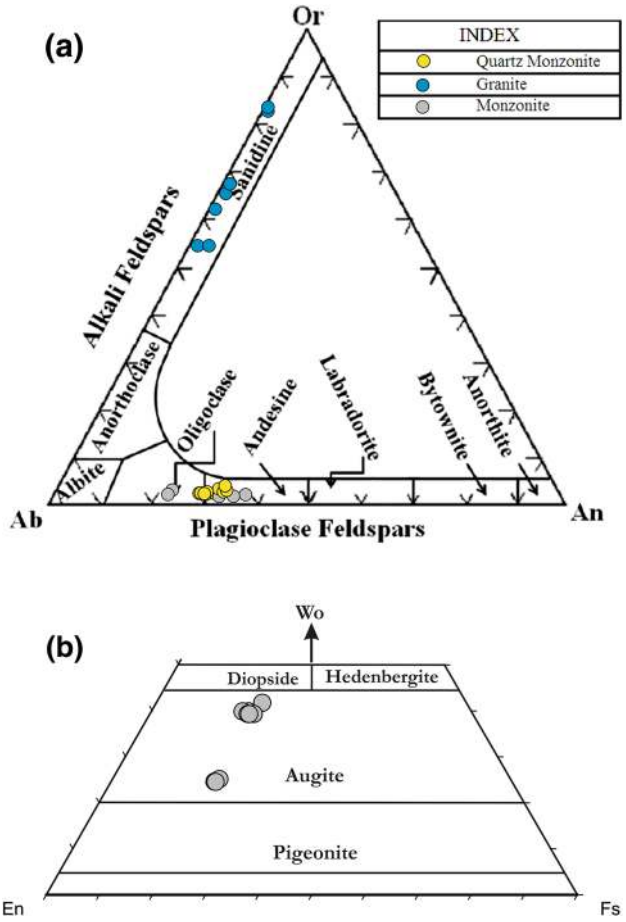

Figure 6: **a** Conventional classification diagram of the feldspars from the quartz monzonite, monzonite and granite, **b** classification diagram of pyroxenes in the monzonite sample.

REE patterns (Fig. 8). The prominent negative Eu anomalies and depleted HREE in the studied samples substantiate the anorogenic nature of the felsic units of PMIC. Loiselle and Wones[36] opined that A-type granitoid contain high K_2O/Na_2O, $Fe/(Fe+Mg)$, K_2O and incompatible trace element concentrations (including REE, Zr, Nb and Ta). Whalen et al.[32] proposed that A-type granitoid contain higher abundance of Al, Mg, Ca, V, Fe, K + Na, Zn, Ga, Nb, Y, Zr and REE (except Eu). In the present study, the K_2O/Na_2O ratios of the monzonite and quartz monzonite samples exhibit ≥ 1 values, whereas the granites and granodiorites exhibit < 1 values. Except granites (Zr: 45.9–72.8 ppm; Nb: 16.7–24 ppm) all other samples (Zr: 116.6–1395 ppm; Nb: 56.1–111 ppm) exhibit relatively higher incompatible element concentrations.

Mantle plume: large columns of hot rocks rising through the mantle. The heat from these plumes causes melting of the lower lithosphere rocks.

The exact mode and mechanisms of formation of the anorogenic granitic intrusions are still not clear. Loiselle and Wones[36] suggested that A-type granitoid was formed by the fractionation of the mantle-derived alkali basalts without crustal interaction. Subsequently, Collins et al.[37] proposed that high temperature, vapor absent melting of residual felsic granulite source may generate an anhydrous melt containing halides and higher amount of highly charged cations such as Zr and REE that are abundant in A-type granitoid. Anderson[38] suggested that partial melting of quartz diorite, tonalite and granodiorite also exhibit a compositional character similar to the A-type granitoids. The crustal component that had undergone a previous partial melting episode along with mantle plume impingement/diapirism in an extensional regime may also contribute to the formation of anorogenic magmatism.[39] According to Frost and frost,[40] the combination of partial melting of crustal rocks and differentiation of basaltic magma, and assimilation of crustal components into the ascending basaltic magma can produce A-type granitoids.

When the samples of the present study are plotted in different A-type granite discrimination

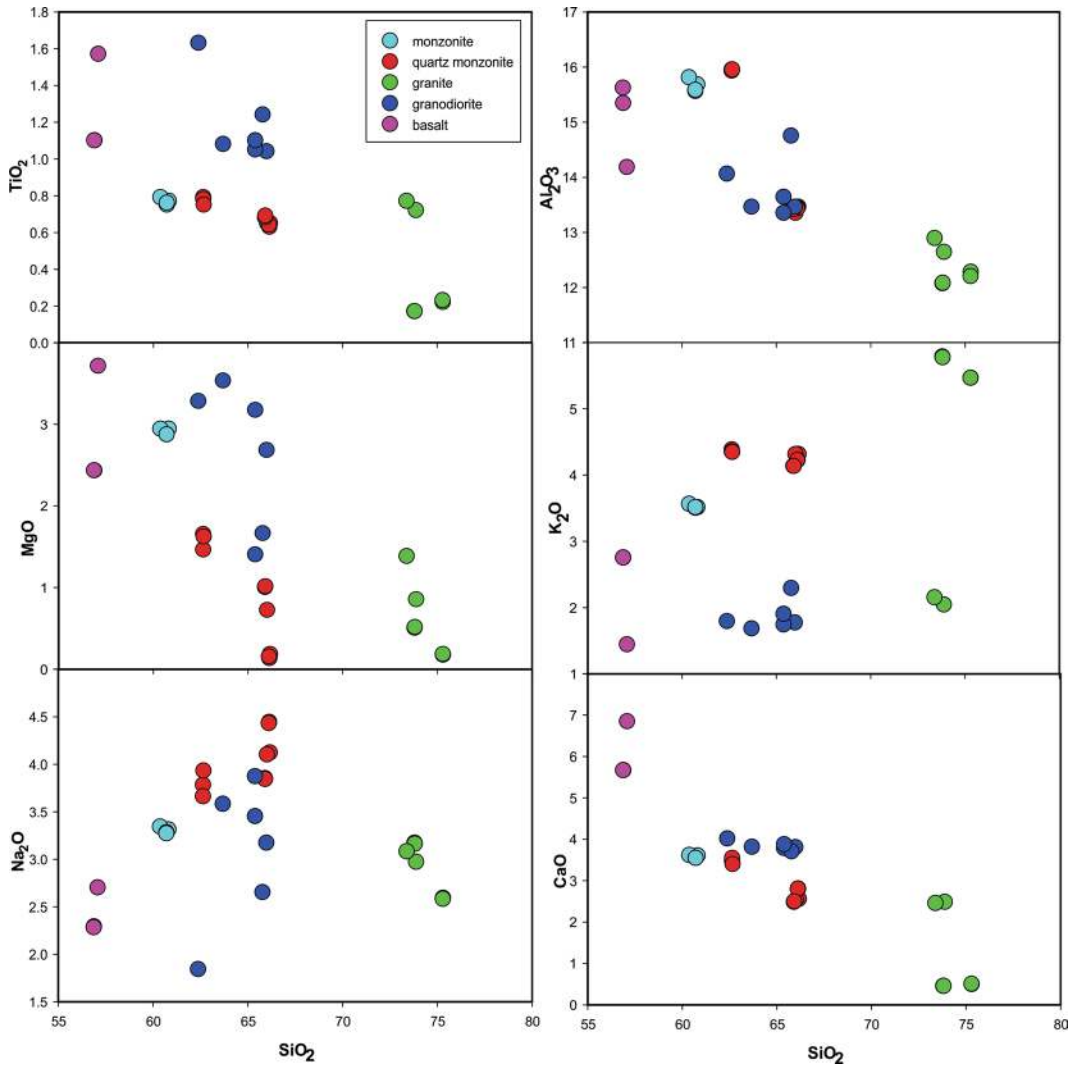

Figure 7: Variation diagram of SiO_2 with other major oxides exhibit definite trend for the mafic and felsic samples except for the granites.

diagrams (Fig. 12), the granites plot in the A2 type granite region whereas the granodiorites, monzonites and quartz monzonites plot in the A1 type granite field. The A2 type granites are widely considered as the product of crustal melting and the genesis A1 type is generally attributed to the fractionation of a basaltic parental melt.[41] The association of A1 and A2 type granites along with mafic rocks clearly point towards a complex magmatic history of the PMIC. Greenberg[42] suggested that evolved anorogenic magmatism and primitive anorogenic magmatism are the two main processes operated for the formation of these type of rocks. The rocks from Phenai Mata complex are having characteristics of evolved anorogenic magmatic rocks, as well as primitive magmatic rocks.

In the variation diagrams with SiO_2 (Fig. 7) the monzonites, quartz monzonites and granodiorites exhibit well-defined trends with the mafic rocks of PMIC indicating that these rocks may be cogenetic in nature. However, the granites of PMIC do not exhibit any geochemical trends with the associated felsic and mafic units. Furthermore, granites exhibit prominent Nb–Ta anomalies in the primitive mantle normalized diagram (Fig. 8), whereas other felsic units do not have negative Nb and Ta anomalies pointing that the granites in this area have a different genesis than the other felsic rock units. However, the A-type granitoids appear to represent crustal growth and/or crustal differentiation during tectonic events generally unrelated to the subduction processes.[41]

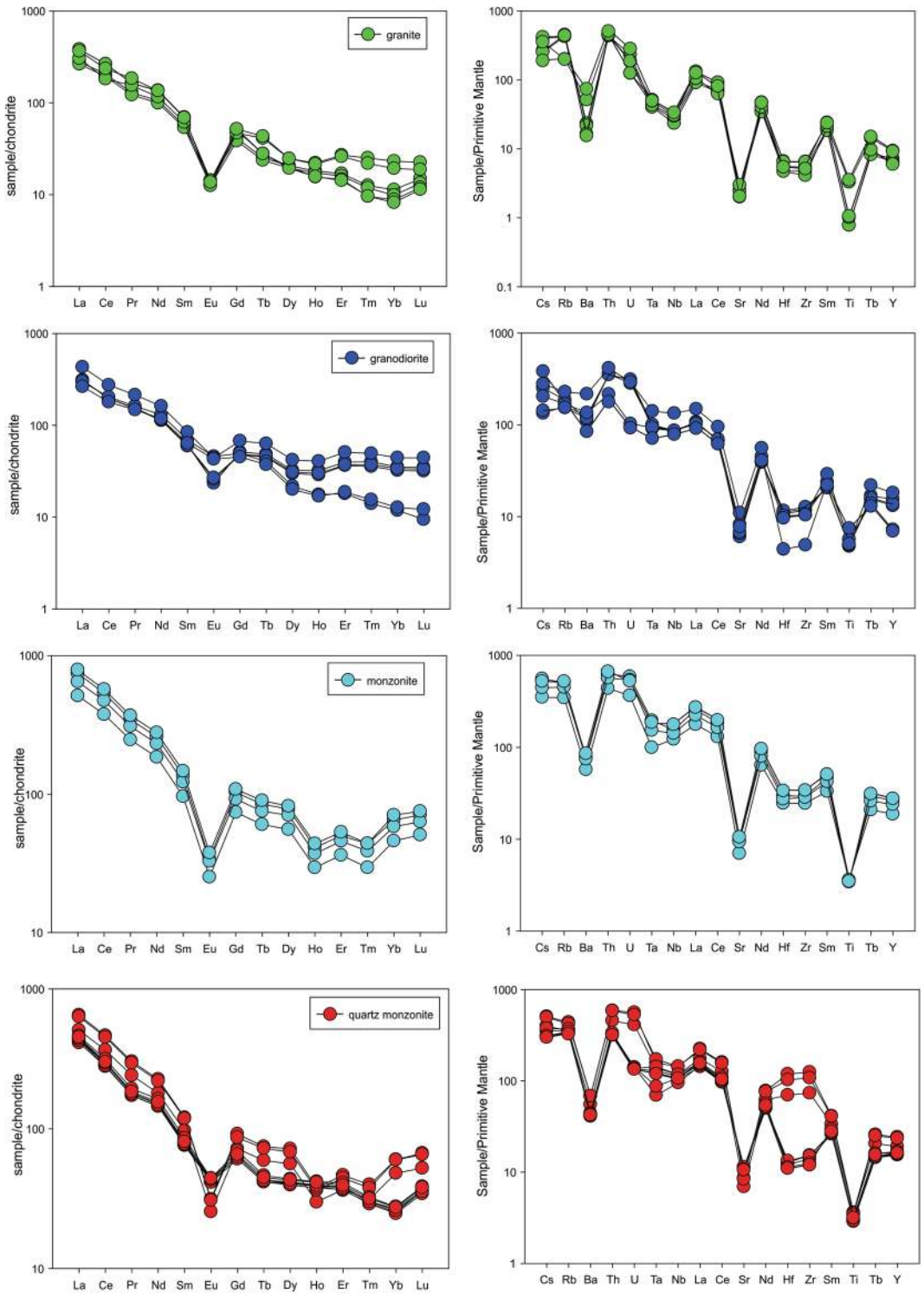

Figure 8: Chondrite normalized REE and Primitive mantle normalized multi element diagrams of **a**, **b** granite, **c**, **d** granodiorite, **e**, **f** monzonite and **g**, **h** quartz monzonite Normalizing values for the chondrite and Primitive mantle are from Sun and McDonough[49].

The field evidence from the PMIC indicates mixing and mingling of at least two contrasting magma compositions in the genesis of these anorogenic intrusions. The A-type granite discrimination diagrams (Fig. 12) clearly demarcates the granites as the A2 type and the other

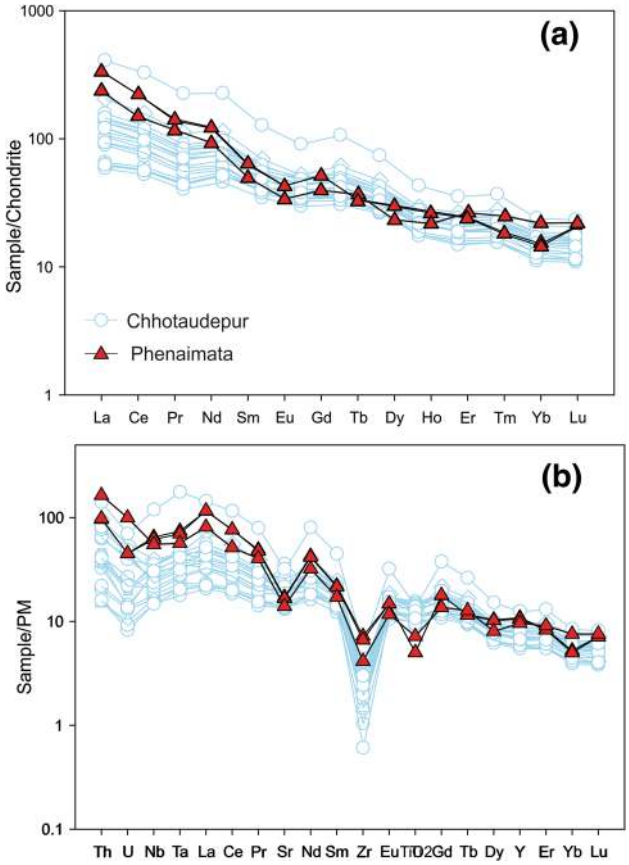

Figure 9: **a** Chondrite normalized REE and **b** primitive mantle normalized multi element diagram of basalts of PMIC. Basalts from the Chhotaudepur province[34] are also given for comparison. Normalizing values for the chondrite and Primitive mantle are from Sun and McDonough[49].

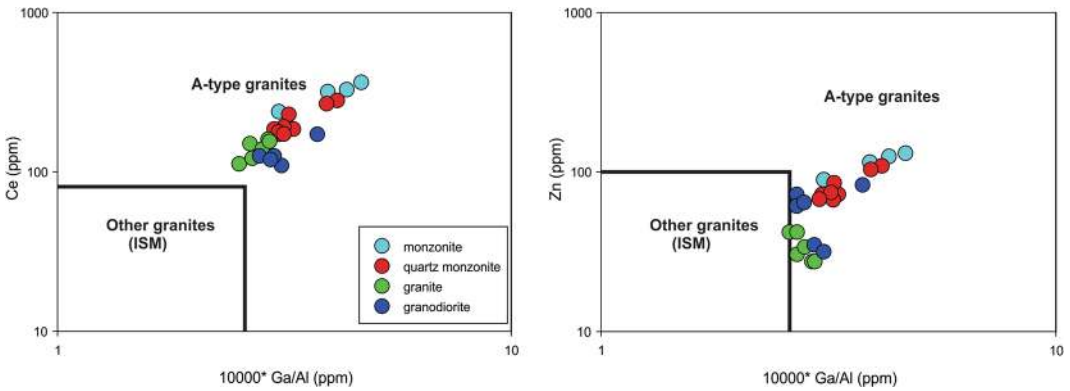

Figure 10: The **a** 1000*Ga/Al vs. Ce and **b** 1000*Ga/Al vs. Zn classification diagrams[32] shows all the felsic samples from the PMIC plot with in the field of A-type granites.

felsic rocks as A1 type. It is clear that multiple magmatic processes which are contemporaneous with the plume event in the DLIP were attributed to the formation of the A-type granites of PMIC. Bonin[41] presented evidence for the generation of A1 type granites from the mantle derived mafic and intermediate magmas. In the generation of the A2 type granites significant amount of crustal components might have been involved.[43–45] Genetic models proposed for the generation of A2 type granites include the crustal melting, partial melting of lower crust felsic granulites which

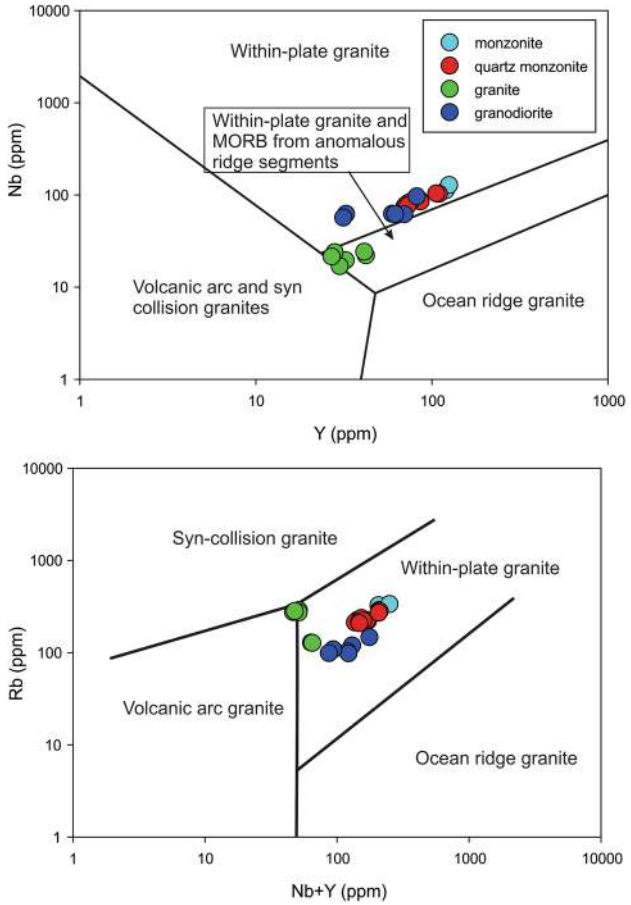

Figure 11: **a** Y (ppm) vs. Nb (ppm) and Nb + Y (ppm) vs. Rb (ppm) tectonic discrimination diagrams indicates a with in plate granite character for the PMIC felsic rocks (after Pearce et al.)[35].

were depleted in the course of earlier melting episodes,[35] melting of meta-igneous,[46] melting of alkali-metasomatized compositions,[47] and involvement of mixed OIB-crust sources.[44, 45]

For the crustal melting process, pounded and underplated basaltic magmas in the DLIP might have supplied the necessary heat for the melting of the upper crust.[48] The continuous/episodic interaction of plume head with the crustal components might have resulted in the partial melting of the granitic basement to form the A2 type granites in the PMIC. At the same time, the fractional crystallization of the basaltic magma would have ultimately resulted in the generation of A1 type granites. It is also possible that the magmas which were stalled at the base of the crust or coalesced into the local magma chambers would have resulted in the crystal fractionation before the injection into the shallow crust.[50] The MMEs, syn-plutonic dykes and hybrid zones which are exposed in the PMIC indicates both A1 and A2 type granites and the basaltic magmas were mixed and mingled at shallow crustal levels before their emplacement.

7 Conclusions

1. The presence of mafic enclaves, syn plutonic dykes, interaction of mafic and felsic magmas at the PMIC point towards a complex magmatic environment for their genesis.
2. All the field and elemental signatures of the felsic rocks from the PMIC exhibit a close proximity to the A-type granites.
3. In the primitive mantle normalized multi-element diagram, granites exhibit negative anomalies at Rb, Ta, Nb, Sr, Hf, Zr, Ti and positive anomalies at Th, La, Nd, and Zr, whereas granodiorite, Monzonite and quartz monzonite exhibit negative anomalies at Ba, Sr, Hf, Zr, and Ti.
4. The geochemical characters of monzonites, quartz monzonites and granodiorites from the PMIC are similar to that of A1 type granites, which is generally considered as a prod-

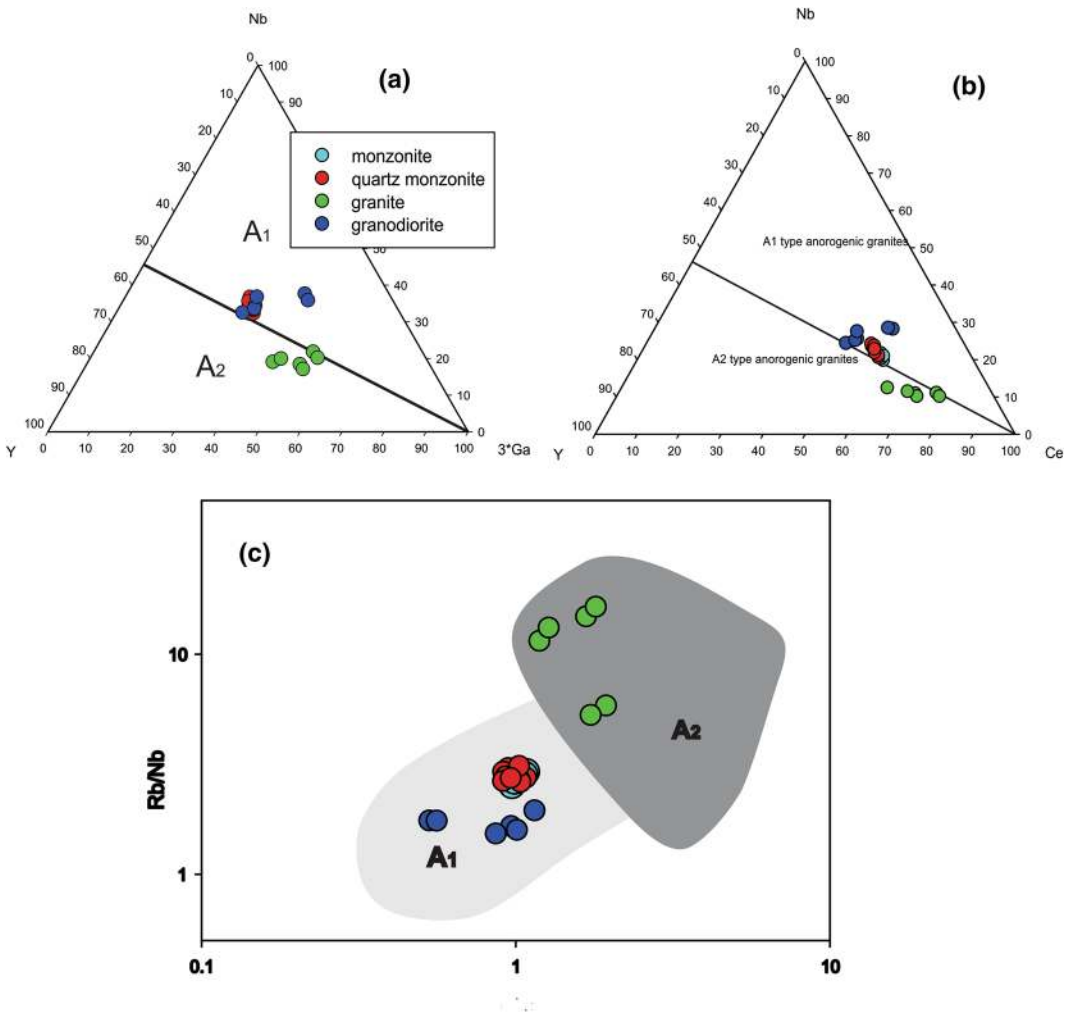

Figure 12: **a** Nb-Y-3*Ga, **b** Y–Nb–Ce and Y/Nb vs. Rb/Na discrimination diagrams for A-type granites of PMIC (From Eby)[45].

uct of fractional crystallization, whereas the granites from the PMIC which exhibit A2 type geochemical characters may be derived by the melting of the pre-existing crust or by the incorporation of the crustal components during the ascent of the magma.

5. The contrasting magmatic signatures of the felsic rocks from the PMIC indicates that the A1 type rocks were derived as a result of fractional crystallisation of basaltic magma, whereas the A2 type might have been derived by the plume-induced crustal melting or by a complex process involving both fractional crystallisation and crustal melting.
6. The field and geochemical evidence from the PMIC indicate that the contrasting felsic magmas and mafic magmas were mixed and mingled at crustal or shallow crustal level to form complex field relationship.

Acknowledgements

The financial support from Department of Science and Technology, New Delhi in the form of a research Grants (ESS/16/295/2006 and ESS/16/301/2006) to KRH and KRR are acknowledged. Prof. N.V Chalapathi Rao is acknowledged for the suggestions and support. We thank Prof. M. Santosh and Prof. Sajeev for their invitation and critical comments. Thanks are due to two anonymous reviewers for their suggestions for improving the manuscript.

Received: 6 April 2018 Accepted: 21 May 2018
Published online: 8 June 2018

References

1. Lightfoot PC, Evans-Lamswood D (2015) Structural controls on the primary distribution of mafic–ultramafic intrusions containing Ni–Cu–Co–(PGE) sulfide

mineralization in the roots of large igneous provinces. Ore Geol Rev 64:354–386
2. Ernst RE (2014) Large igneous provinces. Cambridge University Press, Cambridge
3. Jowitt SM, Ernst RE (2013) Geochemical assessment of the metallogenic potential of Proterozoic LIPs of Canada. Lithos 174:291–307
4. Bryan SE, Ernst RE (2008) Revised definition of large igneous provinces (LIPs). Earth Sci Rev 86(1–4):175–202
5. Xu YG, Chung SL, Shao H, He B (2010) Silicic magmas from the Emeishan large igneous province, Southwest China: petrogenesis and their link with the end-Guadalupian biological crisis. Lithos 119(1–2):47–60
6. Zhang CL, Zou HB (2013) Permian A-type granites in Tarim and western part of Central Asian Orogenic Belt (CAOB): genetically related to a common Permian mantle plume? Lithos 172:47–60
7. Shellnutt JG, Zhou MF (2007) Permian peralkaline, peraluminous and metaluminous A-type granites in the Panxi district, SW China: their relationship to the Emeishan mantle plume. Chem Geol 243(3–4):286–316
8. Bose MK (1972) Deccan basalts. Lithos 5(2):131–145
9. Devey CW, Cox KG (1987) Relationships between crustal contamination and crystallisation in continental flood basalt magmas with special reference to the Deccan Traps of the Western Ghats, India. Earth Planet Sci Lett 84:59–68
10. Hari KR, Nambiar CG, Furuyama K, Rai SK (2002) Some geochemical and petrogenetic relations between flows and dykes of Deccan Trap from Chhaktalao area, Madhya Pradesh. J Geol Soc India 59(3):225–232
11. Burov E, Guillou-Frottier L, d'Acremont E, Le Pourhiet L, Cloetingh SAPL (2007) Plume head–lithosphere interactions near intra-continental plate boundaries. Tectonophysics 434(1–4):15–38
12. Lehmann B, Burgess R, Frei D, Belyatsky B, Mainkar D, Rao NVC, Heaman LM (2010) Diamondiferous kimberlites in central India synchronous with Deccan flood basalts. Earth Planet Sci Lett 290(1):142–149
13. Basu AR, Renne PR, Dasgupta DK, Teichmann F, Poreda RJ (1993) Early and late alkali igneous pulses and a high-3He plume origin for the Deccan flood basalts. Science 261:902–906 **(New York, N.Y.)**
14. Rock NMS, Gwalani LG, Griffin BJ (1994) Alkaline rocks and carbonatites of Amba Dongar and adjacent areas, Deccan Alkaline Province, Gujarat, India. 2. Complexly zoned clinopyroxene phenocrysts. Miner Petrol 51(2):113–135
15. Simonetti SL, Goldstein SS, Schmidberger SG (1998) Viladkar, Geochemical and Nd, Pb, and Sr Isotope Data from Deccan Alkaline Complexes-Inferences for Mantle Sources and Plume-Lithosphere Interaction. J Petrol 39(11–12):1847–1864
16. Ray R, Sheth HC, Mallik J (2007) Structure and emplacement of the Nandurbar–Dhule mafic dyke swarm, Deccan Traps, and the tectonomagmatic evolution of flood basalts. Bull Volcanol 69(5):537
17. Sen G, Bizimis M, Das R, Paul DK, Ray A, Biswas S (2009) Deccan plume, lithosphere rifting, and volcanism in Kutch, India. Earth Planet Sci Lett 277(1–2):101–111
18. Sheth HC, Pande K (2014) Geological and 40Ar/39Ar age constraints on late-stage Deccan rhyolitic volcanism, inter-volcanic sedimentation, and the Panvel flexure from the Dongri area, Mumbai. J Asian Earth Sci 84:167–175
19. Sheth HC, Melluso L (2008) The Mount Pavagadh volcanic suite, Deccan Traps: geochemical stratigraphy and magmatic evolution. J Asian Earth Sci 32(1):5–21
20. Gwalani LG, Rock NMS, Chang WJ, Fernandez S, Allegre CJ, Prinzohofer A (1993) Alkaline rocks and carbonatites of Amba Dongar and adjacent Areas, Deccan Igneous Province. Gujarat, India: Geology, petrography and petrochemistry. Miner Petrol 47:219–253
21. Gwalani LG, Fernandez S, Karanth RV, Demeny A, Chang W-J, Avasia RK (1994) Alkaline and Tholeiitic Dyke Swarm associated with Amba Dongar and Phenai Mata complexes, Chhota Udaipur alkaline sub-province, Western India. Mem Geol Soc India 33:391–424
22. Sukeshwala RN, Avasia RK (1972) Carbonatite-alkalic complex of Panwad-Kawant, Gujarat and its bearing on the structural characteristics of the area. Bull Volcanol 35:564–578
23. Simonetti K, Bell SG (1998) Viladkar, Isotopic data from the Amba Dongar carbonatite complex, West central India: evidence for an enriched mantle source. Chem Geol 122:185–198
24. Kumar S (1996) Geochemical specialization of Phenai Mata Igneous Complex, Baroda district, Gujarat. J Sci Res 46:207–218
25. Kumar S (2003) Variation in the thickness of the lithosphere underneath the Deccan volcanic province, evidence from rare earth elements. Mem Geol Soc India 52:179–194
26. Hari KR, Randive K (2018) Mixing and mingling of dissimilar magmas as against extreme differentiation of tholeiitic magmas: a new insight on the petrogenesis of Phenai Mata Igneous Complex, Deccan Large Igneous Province, India. Indian J Geosci (accepted)
27. Gwalani LG, Fernandez S, Karanth RV, Demeny A, Chang W-J, Avasia RK (1995) Alkaline and tholeiitic dyke swarm associated with AmbaDongar and Phenai Mata complexes, Chhota Udaipur alkaline sub-province, western India. Mem Geol Soc India 33:391–423
28. Hari KR, Rao NVC, Swarnkar V, Hou G (2014) Alkali feldspar syenites with shoshonitic affinities from Chhotaudepur area: implication for mantle metasomatism in the Deccan large igneous province. Geosci Front 5(2):261–276
29. Middlemost EA (1985) Magmas and magmatic rocks: an introduction to igneous petrology. Longman, London, pp 1–266

30. Torab FM, Lehmann B (2007) Magnetite—apatite deposits of the Bafq district, Central Iran: apatite geochemistry and monazite geochemistry. Miner Mag 71:347–367
31. Singh AK, Nayak R, Khogenkumar S, Subramanyam KSV, Thakur SS, Bikramaditya Singh RK, Satyanarayanan M (2017) Genesis and tectonic implications of cumulate pyroxenites and tectonite peridotites from the Nagaland–Manipur ophiolites, Northeast India: constraints from mineralogical and geochemical characteristics. Geol J 52(3):415–436
32. Whalen JB, Currie KL, Chappell BW (1987) A-type granites: geochemical characteristics, discrimination and petrogenesis. Contrib Miner Petrol 95(4):407–419
33. Coleman RG, DeBari S, Peterman Z (1992) A-type granite and the Red Sea opening. Tectonophysics 204(1–2):27–40
34. Hari KR, Rao NC, Swarnkar V (2011) Petrogenesis of gabbro and orthopyroxene gabbro from the Phenai Mata Igneous Complex, Deccan volcanic province: products of concurrent assimilation and fractional crystallization. J Geol Soc India 78(6):501–509
35. Pearce JA, Harris NB, Tindle AG (1984) Trace element discrimination diagrams for the tectonic interpretation of granitic rocks. J Petrol 25(4):956–983
36. Loiselle MC, Wones DR (1979) Characteristics and origin of anorogenic granites. Geol Soc Am Abstr Prog 11:468
37. Collins WJ, Beams SD, White AJR, Chappell BW (1982) Nature and origin of A-type granites with particular reference to southeastern Australia. Contrib Miner Petrol 80(2):189–200
38. Anderson JL (1983) Proterozoic anorogenic granite plutonism of North America. Geol Soc Am Mem 161:133–154
39. Anderson JL, Bender EE (1989) Nature and origin of Proterozoic A-type granitic magmatism in the southwestern United States of America. Lithos 23(1–2):19–52
40. Frost CD, Frost BR (2010) On ferroan (A-type) granitoids: their compositional variability and modes of origin. J Petrol 52(1):39–53
41. Bonin B (2007) A-type granites and related rocks: evolution of a concept, problems and prospects. Lithos 97(1–2):1–29
42. Greenberg JK (1990) Anorogenic granite associations as products of progressive continental evolution. Geol Assoc Can Spec Pap 38:447–457
43. Goodge JW, Vervoort JD (2006) Origin of Mesoproterozoic A-type granites in Laurentia: Hf isotope evidence. Earth Planet Sci Lett 243(3–4):711–731
44. Eby GN (1990) The A-type granitoids: a review of their occurrence and chemical characteristics and speculations on their petrogenesis. Lithos 26(1–2):115–134
45. Eby GN (1992) Chemical subdivision of the A-type granitoids: petrogenetic and tectonic implications. Geology 20(7):641–644
46. Creaser RA, Price RC, Wormald RJ (1991) A-type granites revisited: assessment of a residual-source model. Geology 19(2):163–166
47. Martin RF (2006) A-type granites of crustal origin ultimately result from open-system fenitization-type reactions in an extensional environment. Lithos 91(1–4):125–136
48. Campbell IH (2007) Testing the plume theory. Chem Geol. 241:153–176
49. Sun SS, McDonough WS (1989) Chemical and isotopic systematics of oceanic basalts: implications for mantle composition and processes. Geol Soc Lond Spec Publ 42(1):313–345
50. Krishnamurthy P, Gopalan K, Macdougall JD (2000) Olivine compositions in picrite basalts and the Deccan volcanic cycle. J Petrol 41(7):1057–1069

K. R. Hari is a Professor at School of Studies in Geology and Water Resource Management, Pt. Ravishankar Shukla University, Raipur, Chhattisgarh. His research fields include Large Igneous provinces, dyke swarms, fluid inclusions, alkaline magmatism, super continent tectonics and Early earth evolution.

M. P. Manu Prasanth is a Research scholar at School of Studies in Geology and Water Resource Management, Pt. Ravishankar Shukla University, Raipur, Chhattisgarh. His research interests include greenstone belts, layered igneous complexes, mantle xenoliths and Archean crustal evolution.

Vikas Swarnkar is a consultant at Virinch Earth Spectator, Member of District Expert Appraisal Committee (DEAC), Mining Department, Chhattisgarh and Assistant Professor (guest) at Govt. Digvijay Autonomous P.G. College, Rajnandgaon, Chhattisgarh. He holds Ph.D degree from Pt Ravishankar Shukla University, Raipur, Chhattisgarh, India, His research interest includes mineralogy, igneous petrology and geochemistry.

Jami Vijaya Kumar received his Ph.D from RTM Nagpur University and he is presently working as a Dy.Ore Dressing Officer at Regional Mineral Processing Laboratory. His research interests include Platinum Group Elements (PGE) and Large Igneous Provinces.

Kirtikumar R. Randive is working as Associate Professor at the Post-Graduate Department of Geology, RTM Nagpur University, Nagpur. He was a member of the 31st Indian Scientific Expedition to Antarctica. His research fields include ore geology, Deccan Large Igneous Province, Alkaline magmatism, Environmental and Medical Geology.